Terbit *online* pada laman web jurnal :http://jurnaldampak.ft.unand.ac.id/

Dampak: Jurnal Teknik Lingkungan Universitas Andalas

| ISSN (Print) 1829-6084 |ISSN (Online) 2597-5129|

Artikel Penelitian

Preliminary Feasibility Study of TiO2-Coal Fly Ash Photocatalysts for Simultaneous Organic Pollutant Removal and Qualitative Hydrogen Evolution from Laundry Greywater

Sri Hartuti[1)], Leotrido Pahalatua Nababan[1], Hanggara Sudrajat[2], Nurmeizon Saleh[1].*
[1]*Photochemical Engineering Research Group, Department of Environmental Engineering, Institute of Technology Padang, Padang, Indonesia*
[2]*BRIN Research Center for Quantum Physics, Habibie Science and Technology Park (Puspiptek) Buildings 442 and 720, Serpong, Indonesia*
*Koresponden: amy_srihartuti@yahoo.co.id

Diterima: 22 Mei 2026 Diperbaiki: 13 Juni 2026 Disetujui: 28 Juli 2026

ABSTRACT

Rapid industrialization in Indonesia has increased the generation of coal fly ash (CFA) from coal-fired power plants, while domestic greywater from laundry activities is commonly discharged without adequate treatment. These environmental challenges require integrated and resource-efficient solutions. This study investigates the valorization of CFA as a low-cost support material for TiO_2 photocatalysts synthesized using the sol–gel method to simultaneously degrade organic pollutants and promote hydrogen evolution using real laundry greywater as the reaction medium. CFA was characterized through Loss on Ignition (LOI), X-ray fluorescence (XRF), and slurry pH analysis. Pretreatment involved sequential washing, mild acid neutralization, drying, and calcination prior to sol–gel synthesis. The resulting TiO_2/CFA composite was immobilized on stainless steel using brush coating, calcined at 400°C, and tested in a closed batch reactor under UV irradiation. The greywater was coarsely filtered and adjusted to pH 6.0–7.5 before treatment. Characterization confirmed the suitability of CFA as a catalyst support, with an LOI of 1.66%, SiO_2 content of 47.64%, Al_2O_3 content of 18.17%, and a slurry pH decrease from 11.25 to approximately 8.0 after pretreatment. After six hours of UV irradiation, organic content decreased from 97.9 to approximately 45.1 mg/L, corresponding to an overall removal efficiency of 53.96 ± 0.12%. However, without control experiments, this removal reflects combined effects of photocatalysis, photolysis, and adsorption. An MQ-2 sensor detected reducing gas accumulation under nitrogen-purged anaerobic conditions, but the gas identity remains unconfirmed due to the sensor's non-selectivity and requires verification using GC-TCD. The findings demonstrate the potential of CFA as a functional TiO_2 support for integrated greywater treatment and photocatalytic hydrogen evolution, while quantitative hydrogen analysis and advanced catalyst characterization are recommended for further investigation.

Keyword: Coal fly ash, TiO_2-Based Photocatalyst, Sol–Gel Synthesis, Photocatalytic Hydrogen Evolution, Greywater, Permanganate Index, Organic Degradation.

1. INTRODUCTION

Indonesia's growing energy demand has driven the expansion of coal-fired power generation, resulting in large volumes of coal fly ash as an industrial by-product that poses significant environmental risks if inadequately managed. Concurrently, the increasing volume of domestic wastewater, particularly greywater from laundry activities, which constitutes approximately 60–75% of total household wastewater, continues to be discharged into water bodies without sufficient treatment, contributing to organic pollution and eutrophication of aquatic ecosystems (Mohan et al., 2024). These two environmental challenges, though arising from different sectors, share a common need for sustainable, low-cost, and technically feasible management strategies. Photocatalysis, particularly TiO_2-based systems, has emerged as a promising technology capable of addressing both challenges simultaneously, degrading organic pollutants in greywater while potentially generating hydrogen as a clean energy by-product, with coal fly ash offering a locally abundant and low-cost support material for photocatalyst immobilization.

Coal fly ash is commonly classified as hazardous industrial waste due to its fine particulate nature and the presence of potentially toxic elements, particularly arsenic, which can be mobilized into the aqueous phase in

 Attribution-NonCommercial-ShareAlike 4.0 International.

the presence of dissolved organic matter under both oxic and anoxic conditions, thereby posing risks to water quality and aquatic ecosystems (Deonarine et al., 2021; Hartuti et al., 2017a; Hartuti et al., 2017b; Hartuti et al., 2017c; Hartuti et al., 2025). Consequently, sustainable valorization of coal fly ash remains a critical challenge in environmental engineering. In recent years, coal fly ash has gained increasing attention as a low-cost support material for photocatalysts, owing to its silica–alumina-dominated composition that provides structural stability, a high surface area, and abundant adsorption sites capable of enhancing pollutant–catalyst interactions (Hartuti et al., 2025; Lu et al., 2025; Xie et al., 2025). At the same time, organic-rich wastewater such as greywater can function as a sacrificial electron donor in photocatalytic systems, suppressing electron–hole recombination and thereby enhancing hydrogen evolution efficiency (Aslam et al., 2022; Zhang et al., 2025).

TiO_2 stands out among semiconductor photocatalysts for its well-established attributes of high chemical durability, biological safety, and powerful oxidizing capacity, which originates from the photogenerated reactive oxygen species, particularly hydroxyl radicals (•OH), produced upon ultraviolet light excitation. Despite these advantages, practical application of TiO_2-based systems is hindered by two intrinsic limitations: its restricted photoresponse to the ultraviolet fraction of the solar spectrum, and the rapid recombination of photogenerated charge carriers, both of which substantially diminish quantum efficiency and overall catalytic output (Navidpour et al., 2023). Various strategies have been developed to overcome these limitations, including metal and non-metal doping, heterostructure formation, and the use of support materials to improve photocatalyst dispersion, stability, and charge transfer efficiency. The use of coal fly ash as a support material represents a particularly attractive approach, as it simultaneously addresses solid waste valorization and photocatalyst performance enhancement within a single integrated system (Lu et al., 2025).

Despite growing interest in both coal fly ash valorization and greywater-assisted photocatalytic processes, studies that integrate these two aspects within a single system remain limited. Most existing research has investigated either coal fly ash-derived photocatalysts in model pollutant solutions under controlled conditions, or greywater treatment using conventional photocatalytic systems, without exploring their combined application using real greywater as both the treatment substrate and the electron donor medium for simultaneous hydrogen evolution (Aslam et al., 2022; Zhang et al., 2025). Furthermore, the majority of reported studies have focused on optimized or idealized conditions, leaving a significant gap in baseline performance data for TiO_2–coal fly ash systems operating under real, unoptimized greywater conditions — data that are essential for guiding practical system development at household or communal scales.

Therefore, this study aimed to conduct a preliminary investigation of TiO_2-based photocatalysts supported on coal fly ash, synthesized via a sol–gel method, and to evaluate their performance for simultaneous photocatalytic organic pollutant removal and hydrogen evolution using real laundry greywater as the reaction medium. The novelty of this research lies in the integrated approach of valorizing coal fly ash, an abundant industrial by-product in Indonesia, as a functional TiO_2 photocatalyst support within a greywater-driven photocatalytic system, enabling simultaneous organic degradation and qualitative hydrogen evolution. It is stated at the outset that hydrogen evolution in this work is assessed qualitatively by semiconductor gas sensing only; quantitative determination and chemical identification of the evolved gas are beyond the scope of the present study and are reserved for subsequent research stages. Accordingly, this study is framed as a preliminary feasibility assessment rather than a performance optimization study. To the best of the authors' knowledge, no previous study has reported the combined use of sol–gel-synthesized TiO_2–coal fly ash photocatalysts with real laundry greywater as both the treatment medium and electron donor source for concurrent photocatalytic hydrogen evolution. These findings are intended to provide baseline performance data as a foundation for the development of low-cost, dual-function photocatalytic systems applicable at household or communal scales in Indonesia.

2. METHODS

2.1. Research Design

This study was designed as a laboratory-scale experimental investigation aimed at evaluating the feasibility of coal fly ash-derived TiO_2-based photocatalysts for simultaneous organic pollutant removal and hydrogen evolution using real laundry greywater as the reaction medium. The overall experimental workflow is illustrated in **Figure 1**.

The research primarily relied on quantitative experimental measurements, including organic content parameters, pH values, and material characterization data such as loss on ignition (LOI) and oxide composition determined by X-ray fluorescence (XRF). In addition, qualitative experimental observations were conducted to support the interpretation of system behavior, including visual assessment of photocatalyst layer stability, fouling

phenomena, changes in greywater appearance, and indications of hydrogen gas formation. Hydrogen evolution was identified using an MQ-2 semiconductor-based hydrogen detector; therefore, hydrogen-related results were treated as qualitative indications rather than quantitative production rates.

This study was not intended as a comparative or multivariable optimization experiment. Instead, it focused on an in-depth evaluation of a single TiO_2–coal fly ash photocatalyst system operated using real greywater conditioned to a target pH range of 6.0–7.5 prior to treatment. This approach enabled evaluation of both chemical performance, represented by organic matter degradation, and process-related phenomena, including material stability and gas evolution. The experimental work was conducted from October 2025 to January 2026. Coal fly ash samples were obtained from a coal-fired power plant in Padang City, Indonesia, while greywater samples were collected from a local laundry facility in the same city. Photocatalyst synthesis and photocatalytic experiments were carried out in the Environmental Engineering Laboratory at Institute of Technology Padang, Indonesia. Supporting analyses, including XRF and LOI, were conducted at the Quality Control Laboratory of PT. Semen Padang, Indonesia.

The research design focused on two main analytical aspects:

1. Evaluation of coal fly ash-derived material properties, including initial physicochemical characteristics and changes after pretreatment, to determine its suitability as a photocatalyst support in TiO_2–coal fly ash synthesis.
2. Assessment of photocatalytic performance through measurement of changes in greywater organic parameters before and after photocatalytic treatment following SNI 06-6989.22-2004 (BSN, 2004), accompanied by qualitative identification of hydrogen gas formation.

Comprehensive quantitative hydrogen production analysis and advanced mechanistic characterization of the TiO_2–coal fly ash system are intentionally reserved for subsequent stages of the research roadmap.

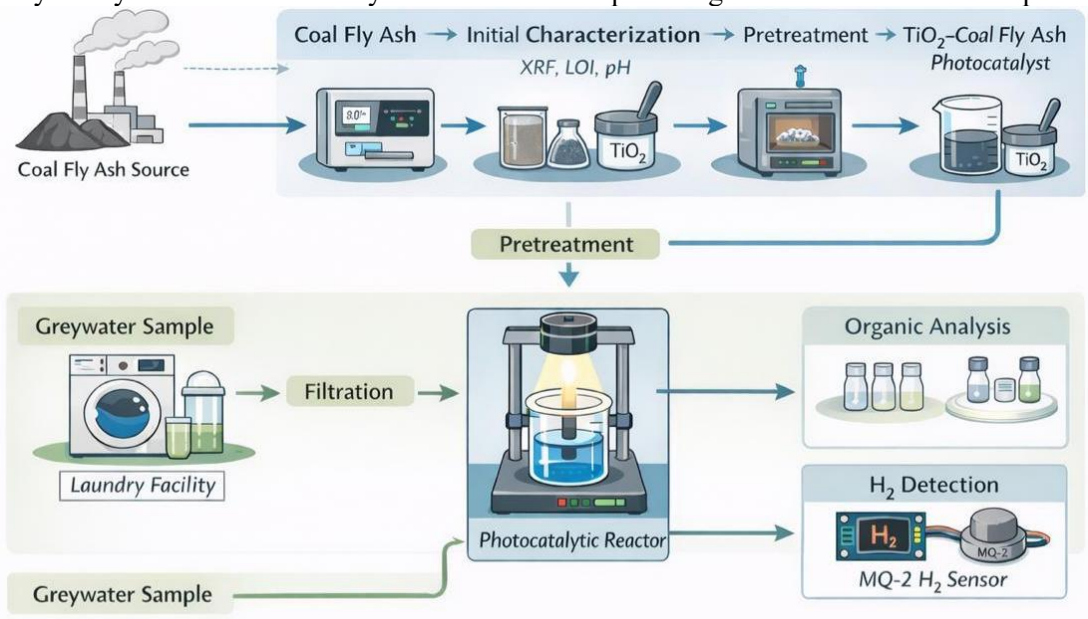


Figure 1. Schematic illustration of the experimental workflow for TiO_2–coal fly ash photocatalytic treatment of greywater, including material characterization, pretreatment, photocatalytic operation, organic analysis, and qualitative hydrogen detection

2.2. Materials and Chemicals

Coal fly ash obtained from a coal-fired power plant in Padang City Indonesia was used as the support material for photocatalyst synthesis. Stainless steel 304 (SS304) plates were used as substrates for immobilization of the TiO_2–coal fly ash photocatalyst during the coating process.

Laundry greywater was collected from a local laundry facility and used as the reaction medium. Prior to use, the greywater was conditioned through the following sequential steps to ensure experimental consistency: (1) homogenization by stirring; (2) pH measurement using a calibrated pH meter; (3) pH adjustment to a target range of 6.0–7.5 using 0.1 N NaOH if pH < 6.0, or 0.1 N HCl if pH > 7.5; and (4) coarse filtration using filter paper to remove large suspended solids. The conditioned greywater was subsequently used without dilution to preserve the real characteristics of the wastewater during photocatalytic experiments. Initial physicochemical

parameters, including pH and organic content, were measured after conditioning to establish baseline conditions.

Titanium tetraisopropoxide (TTIP) was used as the titanium precursor in the sol–gel synthesis process. Ethanol, acetone, deionized water, hydrochloric acid (HCl), and glacial acetic acid were used as solvents and hydrolysis-controlling agents during material preparation and synthesis. Reagents used for organic content analysis, including potassium permanganate ($KMnO_4$), sulfuric acid (H_2SO_4), and oxalic acid, were prepared according to standard analytical procedures.

2.3. Characterization of Raw Coal Fly Ash

Prior to pretreatment and photocatalyst synthesis, raw coal fly ash was characterized to determine its initial physicochemical properties. This characterization step was necessary to establish baseline material conditions and to define an appropriate pretreatment strategy, particularly considering that coal fly ash commonly contains residual carbon, soluble alkaline components, and varying oxide compositions that may influence photocatalyst synthesis and performance.

2.3.1. Loss on Ignition (LOI) Analysis

Thermal gravimetric analysis through LOI measurement was carried out to quantify the fraction of volatile matter and residual unburned carbonaceous material retained within the coal fly ash matrix. This parameter serves as a standard proxy for assessing surface quality and the potential interference of carbonaceous residues with photocatalyst layer deposition.

A known mass of dried fly ash (1 g) was placed in a porcelain crucible and calcined in a furnace at 600°C for 2 hours. This temperature was selected based on the photocatalytic application context of this study, as it is sufficient to combust residual organic matter and unburned carbon relevant to surface chemistry evaluation, while remaining within the thermal stability range of the aluminosilicate framework of the fly ash (Lu et al., 2025). After calcination, the sample was cooled to room temperature in a desiccator and reweighed. The LOI value was calculated based on the mass difference before and after calcination and expressed as a percentage of the initial sample mass.

2.3.2. Oxide Composition Analysis

The oxide composition of coal fly ash was analyzed using X-ray fluorescence (XRF) to evaluate its potential as a catalyst support material, considering the predominance of silica, alumina, and iron oxides in coal combustion byproducts. Before analysis, the coal fly ash was dried at approximately 105°C to eliminate moisture, finely milled, and sieved to achieve a consistent particle size distribution. The produced sample was homogenized and pelletized using a binder to create a compact pellet appropriate for XRF measurement. XRF analysis was performed in oxide mode subsequent to instrument calibration using standard reference materials. The elemental composition was detailed in terms of predominant oxide concentrations, including SiO_2, Al_2O_3, Fe_2O_3, CaO, and other identified oxides, which were utilized to evaluate the appropriateness of coal fly ash as a photocatalyst support.

2.3.3. Slurry pH Measurement

The intrinsic alkalinity of the coal fly ash was evaluated through slurry pH measurement to estimate the influence of soluble alkaline components that may affect subsequent chemical treatment and sol–gel synthesis processes. A coal fly ash–water slurry was prepared by mixing 10 g of coal fly ash with 100 mL of deionized water (1:10 w/v ratio) and stirred for 30 minutes to achieve homogeneity. The pH of the slurry was measured using a calibrated pH meter after stabilization. Measurements were conducted in triplicate, and the average value was reported.

2.4. Pretreatment of Coal Fly Ash

Pretreatment of coal fly ash was conducted to reduce soluble alkaline components, remove residual impurities, and stabilize the surface chemical condition of the material prior to its use as a support in TiO_2 photocatalyst synthesis. Raw coal fly ash characteristically displays pronounced alkaline behavior arising from water-soluble alkali metal oxides (Na_2O, K_2O) and reactive surface silicate–aluminate species; if left unaddressed, these components would disrupt controlled precursor hydrolysis kinetics and impede the formation of a uniform Ti–O–Ti cross-linked network during sol–gel processing.

The pretreatment process comprised three primary phases. The coal fly ash was initially rinsed with warm deionized water to eliminate weakly adhered contaminants and soluble components. Secondly, the solid material underwent acid washing with a 0.1 M HCl solution to diminish surface alkalinity and dissolve remaining alkali oxides. Subsequent to acid neutralization, the material was thoroughly washed with deionized water until a near-neutral rinse pH was attained, in order to eliminate residual acid. Third, the washed material

was dried and then calcined to eliminate residual moisture and enhance material stability before photocatalyst manufacture.

Following pretreatment, slurry pH measurement was performed using the same procedure described in Section 2.3.3 to verify that the surface chemical condition of the coal fly ash had reached a suitable range for TiO_2 sol–gel synthesis. A target post-pretreatment slurry pH of approximately 7.0–8.5 was considered acceptable, consistent with conditions reported to support controlled TiO_2 precursor hydrolysis and homogeneous gel formation (Navidpour et al., 2023; Lu et al., 2025).

2.5. Synthesis of TiO_2–Coal Fly Ash Photocatalyst

The TiO_2–coal fly ash photocatalyst was synthesized using a sol–gel method, in which pretreated coal fly ash served as the catalyst support and titanium tetraisopropoxide (TTIP) was used as the TiO_2 precursor. The synthesis procedure consisted of sol formation, aging, substrate preparation, coating, and stepwise calcination.

A total of 2 g of pretreated coal fly ash, previously dried and adjusted to near-neutral pH, was dispersed in 50 mL of ethanol using a magnetic stirrer at 400 rpm for 1 hour until a homogeneous suspension was obtained. Separately, a precursor solution was prepared by mixing 5 mL of TTIP, 10 mL of ethanol, and 2 mL of glacial acetic acid, then stirring at 300 rpm for 10–15 minutes and allowing the solution to stabilize for 5–10 minutes. Glacial acetic acid was used as a chelating agent to slow the hydrolysis rate of TTIP and promote formation of a more homogeneous and stable sol. The precursor solution was then added dropwise into the coal fly ash suspension at a rate of approximately one drop every 5–10 seconds at 300 rpm to prevent uncontrolled hydrolysis. After precursor addition was completed, 1 mL of deionized water was introduced slowly (approximately one drop every 10–15 seconds) to initiate controlled hydrolysis. The mixture was further stirred for 1 hour to obtain a homogeneous TiO_2–coal fly ash sol, which was subsequently aged for 12 hours at room temperature in a covered container prior to coating.

SS304 plates were pretreated prior to coating to improve surface adhesion. Plate surfaces were mechanically abraded to increase roughness, rinsed with deionized water, and immersed in acetone for 15–30 minutes to remove organic contaminants. Surface activation was performed by immersion in 0.1 M HCl for 5–10 minutes, followed by rinsing with deionized water and ethanol. Plates were then dried at 80°C for 30 minutes, then at 110°C for 30 minutes, and stored in a desiccator for use within 24 hours to avoid surface recontamination.

Coating was performed using a brush coating method by applying the supernatant phase of the aged sol onto the SS304 surface. The first coating layer was dried at 80°C for 30 minutes and cooled to room temperature. The second and third coating layers were applied using the same procedure, followed by drying at 120°C for 30 minutes after each layer. Finally, the coated substrates were calcined through stepwise heating up to 400°C, with a holding time of 1 hour at each stage of 200°C, 300°C, and 400°C. After calcination, samples were cooled naturally inside the furnace to room temperature before use.

It is noted that no post-synthesis characterization of the TiO_2–coal fly ash composite was performed in this study. The formation of a TiO_2 coating layer is supported only indirectly by the observed photocatalytic activity and visual assessment of coating integrity. Direct verification of TiO_2 crystalline phase formation, surface morphology, and elemental distribution through XRD, SEM-EDX, BET, and UV-Vis DRS analyses is identified as a necessary component of subsequent research stages.

2.6. Photocatalytic Experimental Procedure

Photocatalytic experiments were carried out in a closed borosilicate glass batch reactor with a total volume of 2 L, equipped with two UV lamps (UVB type, 25 W each, peak emission wavelength 310 nm, positioned at ±15 cm from the catalyst surface) as the irradiation source. Direct measurement of UV irradiance was not available in our laboratory. Based on the manufacturer's rated UVB output (25 W, peak emission 310 nm) and the lamp-to-catalyst distance of 15 cm, and assuming approximately 15% UV conversion efficiency typical for UVB fluorescent lamps, the estimated irradiance at the catalyst surface is approximately 1.0–1.5 mW/cm^2. This value is presented as a theoretical estimate; direct radiometric measurement using a calibrated UV radiometer is identified as a necessary refinement for subsequent studies. The TiO_2–coal fly ash-coated SS304 plate was installed vertically inside the reactor and positioned to ensure direct and uniform light exposure on the catalyst surface during the reaction.

A total of 2 L of conditioned greywater (pH 6.0–7.5, prepared as described in Section 2.2) was introduced into the reactor, after which the system was tightly sealed to maintain a closed reaction environment. Anaerobic conditions were established by purging the reactor with nitrogen gas (N_2) at a flow rate of 1 L/min under a maximum inlet of 10 psi for 30 minutes prior to initiating irradiation, thereby depleting dissolved oxygen that would otherwise compete with photogenerated electrons as an alternative electron acceptor and inhibit

photocatalytic hydrogen evolution. After purging, the nitrogen flow rate was reduced to 0.1–0.5 L/min to maintain inert conditions throughout the reaction while minimizing stripping of volatile reaction intermediates. The reactor gas outlet was connected to a gas collection bag from the beginning of the experiment to allow continuous collection of gases generated during the photocatalytic process. The photocatalytic reaction was initiated by turning on the UV lamps and allowed to proceed for 6 hours. At the end of the reaction, greywater samples were collected for final organic content analysis, and the collected gas was subjected to qualitative hydrogen identification.

It is acknowledged that no negative control experiments (i.e., greywater under UV irradiation without catalyst, or greywater with catalyst under dark conditions) were conducted in this study. This constitutes a limitation of the current experimental design, as it prevents definitive isolation of the photocatalytic contribution from photolytic degradation or adsorption effects. These control experiments are identified as necessary components of future work to more rigorously quantify the photocatalytic contribution to organic removal.

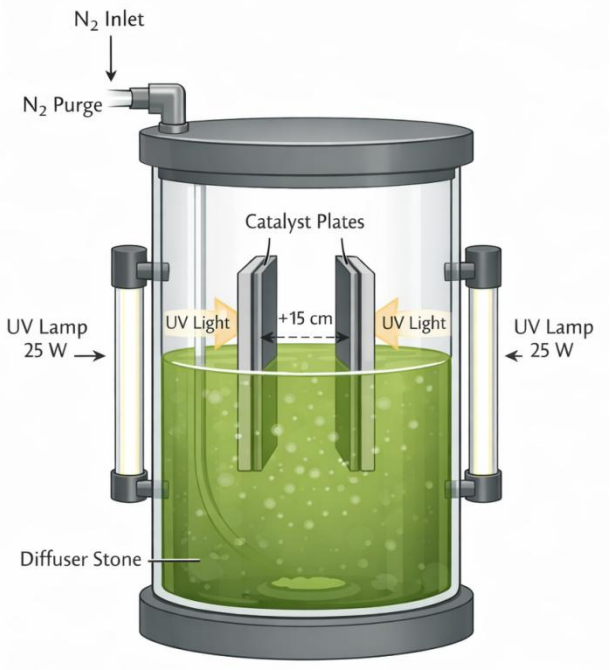


Figure 2. Schematic illustration of the closed borosilicate glass batch reactor used in the photocatalytic experiments, showing the configuration of two UVB lamps (25 W each) positioned on either side of the reactor at a distance of ±15 cm from the catalyst surface, the vertically installed TiO_2–coal fly ash-coated stainless steel catalyst plates positioned at the center of the reactor, the nitrogen (N_2) inlet and purge line at the top, and the diffuser stone at the base of the reactor.

2.7. Analytical Methods

The physicochemical characteristics of greywater were analyzed before and after photocatalytic treatment to evaluate pollutant removal performance. The pH of the samples was measured using a calibrated digital pH meter. Organic content was determined using the permanganate index method following SNI 06-6989.22-2004 (BSN, 2004), in which potassium permanganate ($KMnO_4$) was used as the oxidizing agent under acidic conditions; sulfuric acid (H_2SO_4) and oxalic acid were used during back-titration to determine residual oxidant concentration. Organic content analysis was performed in three independent replicates, with results expressed as the arithmetic mean accompanied by the corresponding standard deviation. Removal efficiency was calculated as:

$$\text{Removal Efficiency (\%)} = [(C_0 - Cf) / C_0] \times 100\% \qquad \text{(Eq. 1)}$$

where C_0 is the initial organic content (mg/L) and Cf is the final organic content after 6 hours of photocatalytic treatment (mg/L).

Statistical analysis was performed using a paired two-tailed Student's t-test to compare organic content before and after treatment, with statistical significance set at $\alpha = 0.05$. Results are reported as mean ± standard deviation together with 95% confidence intervals.

Gas produced during the photocatalytic process was collected in a gas bag connected to the reactor outlet. Qualitative hydrogen identification was performed using an MQ-2 semiconductor-based gas sensor (detection range: 300–10,000 ppm for combustible gases; operating voltage: 5 V DC) integrated with a microcontroller

system. The MQ-2 sensor operates based on resistance changes caused by the adsorption of combustible gases onto its tin oxide (SnO_2) sensing element, producing a measurable change in analog output (ADC value) and resistance ratio (R_s/R_0). Hydrogen evolution in photocatalytic systems has been monitored using low-cost semiconductor-based sensor systems integrated with microcontroller platforms, providing accessible qualitative detection approaches suitable for preliminary investigations (Maaß et al., 2022). In the present study, an MQ-2 semiconductor-based gas sensor — which exhibits high sensitivity to combustible gases including hydrogen, LPG, and methane through resistance changes in its SnO_2 sensing element upon gas exposure — was integrated with a microcontroller system for qualitative hydrogen identification (Sohibun et al., 2021). The sensor was preheated for a minimum of 24 hours prior to use and calibrated against ambient air as the baseline reference. It is acknowledged that the MQ-2 sensor has cross-sensitivity to other combustible gases including methane (CH_4), liquefied petroleum gas (LPG), and carbon monoxide (CO). Therefore, the sensor response observed in this study is interpreted as indicative of the presence of a reducing gas. Hydrogen is the thermodynamically expected product under the applied oxygen-depleted conditions and represents the most plausible attribution; however, stripped volatile organic compounds or, less probably, biogenic methane, cannot be formally excluded as alternative sources. Definitive chemical identification and quantification by GC-TCD or GC-MS are required and constitute the immediate next step of this research.
Supporting material characterization analyses, including XRF and LOI, were conducted at the Quality Control Laboratory of PT. Semen Padang and used as complementary characterization data.

3. RESULTS AND DISCUSSION

3.1. Material Characteristics of TiO_2–Coal Fly Ash Photocatalyst

The physicochemical characteristics of coal fly ash were evaluated prior to synthesis to determine its chemical composition, residual carbon content, and surface chemical properties, as well as to assess its suitability as a support material for TiO_2 immobilization. The characterization results provide essential information regarding the stability of the aluminosilicate framework, surface cleanliness, and chemical environment of the coal fly ash, which collectively influence the interaction between TiO_2 precursors and the support during the sol–gel synthesis process. It should be noted that characterization in this study was limited to the raw and pretreated coal fly ash prior to synthesis. The synthesized TiO_2–coal fly ash composite was not subjected to post-synthesis characterization; therefore, all statements regarding the composite structure and TiO_2 layer formation are inferred from the precursor properties and synthesis conditions rather than directly demonstrated.

3.1.1.Oxide Composition of Coal Fly Ash

X-ray fluorescence (XRF) analysis was conducted to determine the oxide composition of the coal fly ash and to evaluate its appropriateness as a support for TiO_2 photocatalyst synthesis. The oxide composition of coal fly ash influences structural stability, surface properties, acidity–basicity characteristics, and the interaction between the support material and the TiO_2 precursor during the sol–gel process. **Table 1** lists the major oxide composition of the coal fly ash sample.

Table 1. Oxide composition of coal fly ash determined by XRF analysis

No.	Oxide Component	Content (wt.%)
1	SiO_2	47.64
2	Al_2O_3	18.17
3	Fe_2O_3	7.69
4	CaO	4.96
5	MgO	2.08
6	Na_2O	1.47
7	K_2O	0.57
8	Others (minor oxides and undetected components)	~17.42

The XRF results indicate that the coal fly ash is predominantly composed of silica–alumina phases, with SiO_2 and Al_2O_3 accounting for approximately 65.81 wt.% of the total composition. The high SiO_2 content (47.64%) suggests the presence of a stable silicate framework that provides an inert and structurally stable surface for TiO_2 immobilization. High silica content has been reported to enhance catalyst dispersion and maintain structural stability during photocatalytic reactions (Lu et al., 2025; Zhang et al., 2025).
The Al_2O_3 content of 18.17% contributes to thermal and mechanical stability while also providing Lewis acid adsorption sites for organic molecules. This characteristic is beneficial in heterogeneous photocatalysis, as adsorption of pollutants near active TiO_2 sites may enhance photocatalytic oxidation efficiency through a

combined adsorption–photocatalysis mechanism. The combined presence of SiO_2 and Al_2O_3 indicates a typical aluminosilicate structure widely reported as suitable for catalyst support applications (Lu et al., 2025).

Fe_2O_3 was detected at 7.69%, which may influence photocatalytic behavior depending on its concentration and interaction with TiO_2. At moderate concentrations, iron species can act as electron traps, contributing to improved charge separation and mildly extended light absorption into the visible region; however, excessive Fe^{3+} concentrations are known to promote electron–hole recombination through a competing trapping mechanism, thereby reducing photocatalytic activity (Lu et al., 2025). The Fe_2O_3 level observed in this study falls within a moderate range that is more likely to provide beneficial effects on charge separation without significantly suppressing photocatalytic activity.

The CaO content of 4.96% indicates that the coal fly ash can be classified as low-calcium fly ash, commonly associated with Class F characteristics as defined by ASTM C618 (ASTM International, 2022). Low-calcium fly ash is generally considered more chemically stable and suitable as a catalyst support due to the dominance of silica–alumina phases. Lower calcium content also reduces the likelihood of calcium-based deposits and inorganic fouling during photocatalytic applications involving greywater containing surfactants and organic compounds (Mohan et al., 2024; Lu et al., 2025).

Minor oxides including Na_2O (1.47%), K_2O (0.57%), and MgO (2.08%) were also detected. Although present in relatively small amounts, these soluble alkaline oxides contribute significantly to the surface alkalinity of raw coal fly ash, as reflected in the high initial slurry pH discussed in Section 3.1.3. Their removal through pretreatment is therefore an important step in preparing coal fly ash as a suitable TiO_2 support material. The remaining ~17.42 mW/cm² comprises minor oxides below the reliable detection threshold of the instrument and trace elements not reported individually, consistent with typical XRF analysis practice for complex aluminosilicate matrices (ASTM International, 2022).

Overall, the chemical composition of the coal fly ash, dominated by stable silica–alumina phases with low CaO content, supports its utilization as a suitable support material for TiO_2-based photocatalysts intended for simultaneous pollutant removal and hydrogen evolution from greywater

3.1.2.. Loss on Ignition (LOI) Analysis

Loss on Ignition (LOI) analysis was conducted to determine the mass fraction lost during high-temperature heating, which is generally associated with unburned carbon, volatile compounds, and residual organic matter present in coal fly ash. In photocatalyst synthesis, the LOI value is an important indicator because excessive residual carbon may interfere with TiO_2 layer formation, reduce coating homogeneity, and limit the interaction between sol–gel precursors and the coal fly ash surface. **Table 2** presents the LOI value of the coal fly ash sample.

Table 2. Loss on ignition value of coal fly ash sample

Sample	Temperature (°C)	Holding Time (h)	LOI (%)
Coal Fly Ash	600	2	1.66

The measured LOI value of 1.66% indicates a relatively low residual carbon content. This value is consistent with the typical characteristics of Class F fly ash, which generally exhibits LOI values below 6% due to more complete combustion processes (ASTM International, 2022). A low LOI value is beneficial for photocatalyst preparation because it promotes better precursor–surface interaction during the sol–gel process, improves coating adhesion, and enhances structural stability during calcination, as excessive carbon residues have been reported to hinder homogeneous TiO_2 network formation and induce structural instability during thermal treatment (Lu et al., 2025; Zhang et al., 2025).

Overall, the low LOI value confirms that the coal fly ash used in this study possesses suitable initial characteristics for TiO_2 immobilization and supports the formation of stable photocatalyst coatings.

3.1.3.Slurry pH of Coal Fly Ash Before and After Pretreatment

Slurry pH measurement was conducted to evaluate the surface chemical characteristics of coal fly ash, particularly its alkalinity, which may influence the stability of the TiO_2 sol–gel synthesis process. **Figure 3** presents the slurry pH values before and after pretreatment.

As shown in **Figure 3**(a), the raw coal fly ash exhibited strongly alkaline behavior with an average slurry pH of 11.25. This high alkalinity is primarily attributed to the presence of soluble alkali oxides (Na_2O and K_2O), hydration of MgO, and dissociation of silicate–aluminate surface groups commonly found in coal fly ash materials, rather than to its relatively low CaO content (4.96%). Highly alkaline conditions have direct implications for the TiO_2 sol–gel process, as alkaline environments (pH > 9) may induce rapid and uncontrolled hydrolysis of the TTIP precursor, leading to particle agglomeration, reduced coating homogeneity, and weakened TiO_2 adhesion on the support surface (Navidpour et al., 2023).

The pretreatment process, comprising repeated warm water washing, mild acid neutralization using 0.1 M HCl, followed by drying and calcination, successfully reduced the average slurry pH to approximately 7.99–8.03, as shown in Figure 3(b). This near-neutral pH is consistent with the surface chemistry requirements for controlled TiO_2 formation. At pH values close to the point of zero charge of TiO_2 (pH_pzc ≈ 6.0–6.8), surface charge conditions remain relatively stable, facilitating precursor adsorption and promoting more homogeneous TiO_2 layer formation (Navidpour et al., 2023). Overall, the pretreatment strategy effectively improved the physicochemical appropriateness of coal fly ash as a support for TiO2, providing a reliable chemical foundation for the photocatalytic performance discussed in subsequent sections. The reduction in slurry pH from 11.25 ± 0.015 to 8.01 ± 0.021 following pretreatment was statistically significant ($t = 217.8$, $p = 2.67 \times 10^{-9}$), confirming the effectiveness of the applied acid-neutralization protocol.

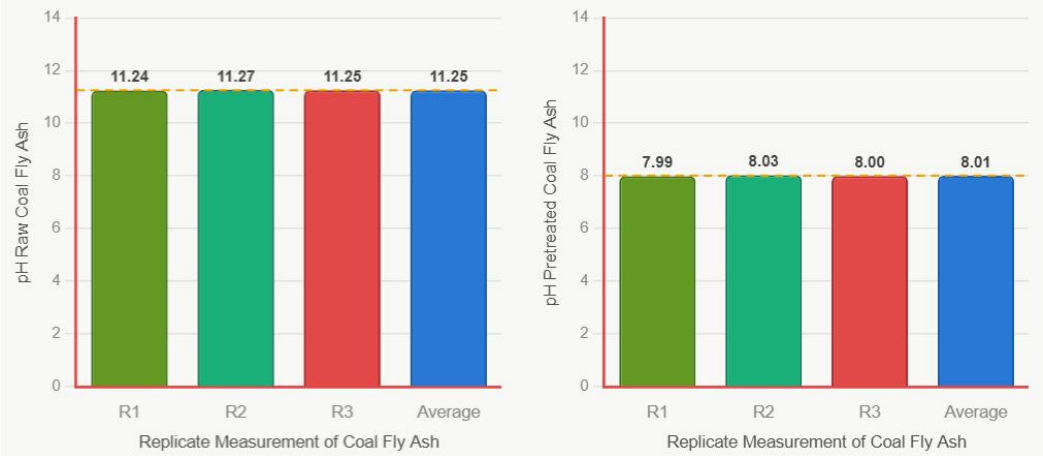


Figure 3. pH values of coal fly ash slurry (a) prior to and (b) following pretreatment.

3.2. Pollutant Removal Performance

The permanganate index (organic number) was used as the primary parameter to evaluate the effectiveness of the TiO_2–coal fly ash photocatalyst in degrading organic compounds present in greywater, measured using the $KMnO_4$ titrimetric method following SNI 06-6989.22-2004 (BSN, 2004). **Figure 4** presents the organic content values before and after photocatalytic process across three replicate measurements.

The results showed that the organic number decreased from an initial average of 97.90 ± 0.01 mg/L to a final average of 45.08 ± 0.12 mg/L after 6 hours of UV irradiation, corresponding to a mean apparent overall removal efficiency of 53.96 ± 0.12% (95% CI: 53.65–54.26%). The mean reduction was 52.828 mg/L (95% CI: 52.543–53.113 mg/L), and the result was statistically significant (paired t-test: $t = 798.1$, $df = 2$, $p = 1.57 \times 10^{-6}$). The narrow standard deviation across triplicate measurements indicates good experimental reproducibility, although it does not address systematic uncertainty arising from the absence of control experiments. This reduction demonstrates that the integrated TiO_2–coal fly ash system was capable of substantially lowering the dissolved organic fraction of real laundry greywater under the applied experimental conditions.

The overall removal efficiency of 53.96% obtained in this study is lower than values typically reported for TiO_2-based photocatalytic systems treating single-component model pollutants, which commonly exceed 80–90% under optimized conditions. Several factors account for this difference. First, the present study employed real laundry greywater rather than a synthetic single-pollutant solution; real greywater contains a complex mixture of surfactants, builders, optical brighteners, oils, and suspended colloids, which compete for •OH radicals, scatter incident photons, and progressively foul the catalyst surface. Second, the photocatalyst was immobilized on a fixed plate rather than suspended as a slurry, substantially reducing the accessible active surface area per unit reactor volume and introducing external mass-transfer limitations. Third, no operational optimization was performed; catalyst loading, irradiation intensity, initial pH, and reaction time were fixed at baseline values. Fourth, the system was operated under oxygen-depleted conditions to favor proton reduction, which simultaneously suppressed the O_2-mediated superoxide pathway that normally contributes to oxidative degradation. The efficiency reported here should therefore be interpreted as a conservative baseline for an unoptimized, immobilized system operating on a real waste stream, rather than as the attainable maximum for this material.

Mechanistically, the degradation of organic compounds in TiO_2-based photocatalysis proceeds through the generation of electron–hole pairs (e^-_CB / h^+_VB) upon UV irradiation with photon energy equal to or exceeding the band gap of TiO_2 (approximately 3.2 eV for anatase). The photogenerated holes (h^+_VB) possess strong oxidative potential and are capable of oxidizing organic compounds either directly or indirectly through the formation of hydroxyl radicals (•OH) via reaction with water molecules or surface hydroxyl groups:

$$h^+_VB + H_2O \rightarrow \bullet OH + H^+ \qquad \text{(Eq. 2)}$$

The generated •OH radicals, being non-selective and highly reactive, subsequently attack organic molecules present in greywater, including surfactants, detergent residues, and colorants, breaking them down into simpler intermediate compounds and ultimately into CO_2 and H_2O (Wu et al., 2021):

$$\bullet OH + \text{Organic compounds} \rightarrow \text{Intermediates} \rightarrow CO_2 + H_2O \qquad \text{(Eq. 3)}$$

The observed removal efficiency can also be attributed in part to the role of coal fly ash as the supporting matrix. The silica–alumina composition of coal fly ash provides adsorption sites that enhance the interaction between organic molecules and the TiO_2 surface, thereby increasing degradation probability through a combined adsorption–photocatalysis mechanism. Previous studies on coal fly ash-supported photocatalysts have reported improved catalyst immobilization stability and enhanced pollutant–catalyst contact due to the aluminosilicate structure (Lu et al., 2025).

Coating integrity was assessed by visual inspection of the SS304 plate before and after each 6-hour run. No macroscopic delamination, flaking, or visible detachment of the coating was observed, and the greywater showed no visible increase in particulate turbidity attributable to catalyst loss. It is acknowledged, however, that visual inspection is insufficient to exclude micro-scale particle release

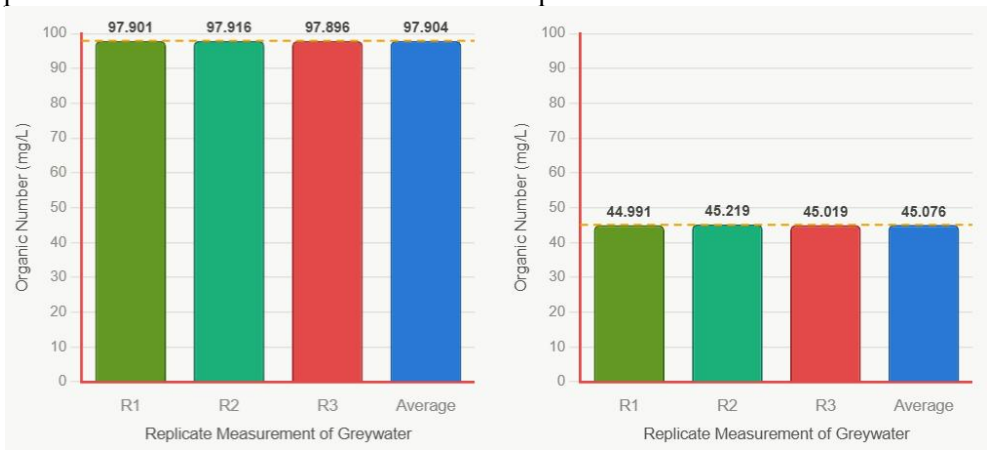


Figure 4. Organic content values (a) prior to and (b) following 6 hours of treatment in the integrated TiO_2–coal fly ash/UV system

It must be emphasized that the measured value of 53.96 ± 0.12% represents the apparent overall removal efficiency of the integrated system under the applied conditions, and should not be interpreted as the photocatalytic contribution alone. In the absence of control experiments, three mechanisms may have contributed concurrently: (i) photocatalytic oxidation mediated by •OH radicals, (ii) direct UV photolysis of chromophoric and unsaturated organic constituents, and (iii) physical adsorption onto the silica–alumina surface of the coal fly ash support. Their relative contributions cannot be deconvoluted from the present dataset. Accordingly, all performance statements in this manuscript refer to the integrated system rather than to photocatalysis in isolation. A full factorial control experiment set is identified as a necessary component of future work.

Table 3. Comparison of organic pollutant removal efficiency of TiO_2-based photocatalytic systems reported in selected studies.

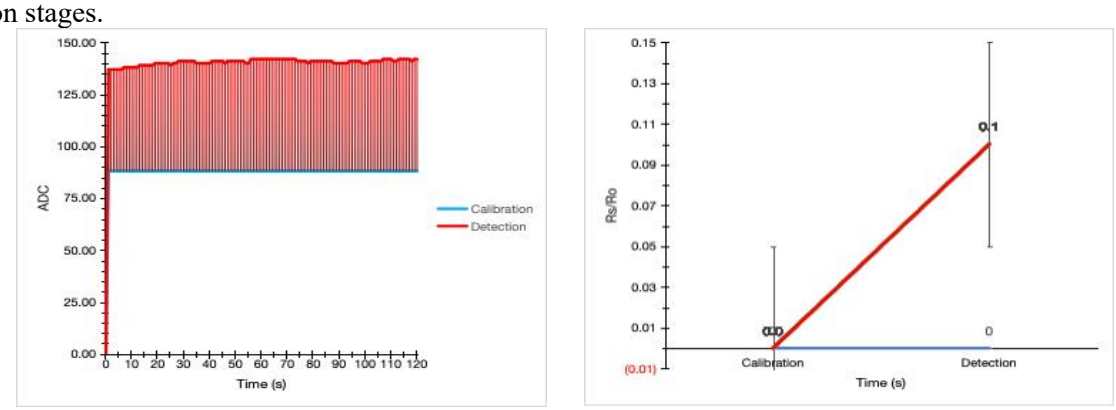
Study	Photocatalyst	Wastewater / Pollutant	Reactor & Light Source	Removal Efficiency	Notes
This study	TiO_2–coal fly ash (immobilized, sol–gel)	Real laundry greywater (complex matrix)	Closed batch, immobilized plate, 2 L, UVB 25 W	53.96 ± 0.12% (permanganate index), 6 h	Unoptimized baseline system; real complex wastewater; O_2-depleted conditions; no control experiments; apparent overall system efficiency (photocatalysis + photolysis + adsorption combined)
Sanchez et al. (2010)	TiO_2 P-25 (Evonik Degussa)	Real hotel + laundry greywater	Batch cylindrical glass photoreactor, 1.0 L, Hg lamp (200–700 nm)	65% DOC removal, 150 min	Real greywater; optimized catalyst concentration; anionic surfactants completely removed; slurry system (higher catalyst–solution contact than immobilized)
Boyjoo et al. (2012)	TiO_2 (Sigma-Aldrich)	Real shower water	Pilot-scale reactor, 31 L, UV mercury lamp (800 W)	~57% TOC removal, 6.5 h	Real greywater; optimized conditions (pH = 3, catalyst 0.07 g/L, air flow 1.8 L/min); slurry system; closest duration to this study (6.5 h vs 6 h)
Wu et al. (2021)	Co_3O_4/{001}/{101}-TiO_2 nanosheets (TC)	Synthetic pharmaceutical wastewater (ENR, CIP, IBU; 10–100 mg/L)	Sealed slurry batch, 250 mL Pyrex flask, 300 W Xe lamp ($\lambda > 400$ nm)	~80% TOC removal (ENR 10 ppm, 60 min); ~100% degradation rate	Highly optimized nanostructured catalyst; single model pollutant; visible light; slurry system; quantitative H_2 confirmed by GC-TCD (~2400 µmol/g in 60 min with TCP)
Kanakaraju et al. (2020)	Base-FA/Cu/TiO_2 (fly ash from sago mill combustion, alkali-modified; sol–gel + wet impregnation)	Synthetic dye wastewater (methyl orange, 10 ppm)	Beaker, 100 mL MO solution, 1.5 g/L catalyst dosage; UVA (λ = 365 nm) or visible light (Opple, 4.5 W); 30 min dark adsorption + 120 min irradiation (150 min total)	100% removal (complete) under UV 99.1% removal under visible light	Synthetic single-dye system, not real complex wastewater; dark adsorption alone contributed ~60–80% of total removal efficiency (across rFA/base-FA samples); acid-modified FA performed worst of the three modification routes; base-FA/Cu/TiO_2 outperformed pristine TiO_2 (81.8% UV / 6.7% visible), especially under visible light; much shorter total duration (150 min) than this study (6 h) and small bench-scale volume (100 mL) vs. this study's 2 L closed batch system.

Note: Efficiency values for literature studies are reported as approximately stated or ranged in the original publications. Direct numerical comparison should be interpreted with caution given differences in pollutant type, concentration, reactor configuration, catalyst loading, and operational conditions.

3.3. Hydrogen Evolution: Qualitative Evidence

To evaluate the occurrence of reductive reactions within the photocatalytic system, the experiment was conducted for 6 hours in a closed reactor under a continuous low nitrogen flow rate (0.1–0.5 L/min) following an initial 30-minute N_2 purging period. Nitrogen purging was applied to minimize dissolved oxygen, which could otherwise act as a competitive electron acceptor and suppress photogenerated electron availability for reduction reactions. The produced gas was directed continuously into a gas collection bag connected to the reactor outlet.

Visual observation indicated gradual expansion of the gas bag volume throughout the reaction period, suggesting continuous gas generation. Qualitative gas identification was performed using an MQ-2 semiconductor-based gas sensor integrated with a microcontroller system. The sensor was preheated for a minimum of 24 hours prior to use and calibrated against ambient air as the baseline reference. **Figure 5** presents the sensor output response (ADC value) and resistance ratio (R_s/R_0) during calibration and gas detection stages.



(a) (b)

Figure 5. Qualitative response of MQ-2 sensor during reducing gas detection in the photocatalytic system: (a) sensor output response (ADC value) as a function of time during calibration and gas detection stages, and (b) comparison of R_s/R_0 ratio between baseline (calibration) and gas exposure conditions.

The sensor response demonstrates only the accumulation of a reducing or combustible gas species in the reactor headspace. Hydrogen is the mechanistically expected product under the applied conditions, but stripped volatile organic compounds and, less probably, biogenic methane, cannot be excluded as alternative or contributing sources on the basis of the present data. Biogenic methane formation is considered unlikely given the short reaction duration of 6 hours, the strongly biocidal UV-B irradiation applied throughout the experiment, and the aerobic origin of the greywater sample without deliberate inoculation of methanogenic microorganisms; however, it cannot be formally excluded in the absence of gas chromatographic analysis. Chemical identification by GC-TCD or GC-MS is required and constitutes the immediate next step of this research. All hydrogen-related findings reported in this study should therefore be regarded as preliminary and hypothesis-generating rather than confirmatory.

3.4. Photocatalytic Mechanism: Integrated Oxidation–Reduction Pathways

The photocatalytic performance of the TiO_2–coal fly ash system revealed two concurrent phenomena: a substantial reduction in organic content (Section 3.2) and qualitative detection of a reducing gas during irradiation (Section 3.3). These observations suggest that oxidation and reduction processes occurred simultaneously at the photocatalyst surface, driven by the spatial separation of photogenerated charge carriers. The fundamental charge-transfer mechanism of TiO_2 under UV irradiation is described as follows:

$$TiO_2 + h\nu \rightarrow e^-_CB + h^+_VB \quad \text{(Eq. 4)}$$

where e^-_CB represents photogenerated electrons in the conduction band and h^+_VB represents holes in the valence band. The generation, separation, and migration of these charge carriers initiate surface redox reactions, and their efficiency strongly determines overall photocatalytic activity (Sudrajat et al., 2021).

Oxidation Pathway

The photogenerated holes (h^+_VB) react with water molecules or surface hydroxyl groups to generate highly reactive hydroxyl radicals, which subsequently degrade complex organic molecules present in greywater into intermediate products and eventually mineralized species (CO_2 and H_2O), as described in Section 3.2. The progressive decomposition of organic constituents in greywater, as evidenced by the significant decrease in

permanganate index, confirms the active operation of this oxidative pathway throughout the 6-hour irradiation period (Sudrajat et al., 2021).

Reduction Pathway

Simultaneously, electrons accumulated in the conduction band participate in reduction reactions. Under nitrogen-purged conditions, dissolved oxygen is minimized, thereby suppressing the competitive oxygen reduction reaction ($O_2 + e^-_CB \rightarrow O_2^{\bullet-}$). This environment enhances the likelihood that conduction-band electrons react with protons present in the aqueous medium to produce hydrogen gas:

$$2H^+ + 2e^-_CB \rightarrow H_2 \quad \text{(Eq. 5)}$$

The importance of prolonged electron lifetime and suppressed recombination in promoting photocatalytic proton reduction has been systematically demonstrated in modified TiO_2 systems (Sudrajat et al., 2023).

Role of Organic Compounds as Hole Scavengers

Organic compounds present in greywater function not only as degradation targets but also as hole scavengers. By reacting with photogenerated holes (h^+_VB), organic species suppress electron–hole recombination, thereby extending the lifetime of conduction-band electrons and increasing their availability for proton reduction. This dual role, as both a pollutant subject to oxidative degradation and a sacrificial electron donor enhancing reductive hydrogen evolution, makes greywater a particularly promising reaction medium for integrated photocatalytic treatment and energy recovery (Xie et al., 2025; Zhang et al., 2025).

The role of organic compounds as hole scavengers in photocatalytic systems has been substantiated by recent mechanistic investigations. Zhang et al. (2025) demonstrated that organic pollutants susceptible to attack by •OH radicals, including reactive dyes and azo compounds, can effectively serve as sacrificial hole consumers, thereby suppressing electron–hole recombination and enhancing photogenerated electron availability for proton reduction. Their study revealed that only pollutants primarily degraded via •OH radical pathways, rather than through superoxide radical ($\bullet O_2^-$) pathways, are capable of promoting H_2 evolution, as the formation of $\bullet O_2^-$ radicals competes directly with proton reduction for conduction-band electrons. This mechanistic principle is consistent with the observations in the present study, where dissolved organic compounds in laundry greywater, including surfactants and detergent residues susceptible to •OH attack, are proposed to function simultaneously as degradation targets and as hole scavengers that suppress recombination and enhance electron availability for the reductive pathway. The qualitative reducing gas signal detected in the present study is therefore mechanistically supported by this hole-scavenging role of greywater organics, even though quantitative H_2 confirmation remains pending.

Contribution of Coal Fly Ash Support

Coal fly ash serves as a supporting matrix that enhances photocatalytic performance through multiple mechanisms. Its silica–alumina composition increases the effective surface area available for TiO_2 deposition, provides adsorption sites for organic molecules, and strengthens interfacial contact between pollutants and TiO_2 active sites, thereby facilitating charge transfer and improving overall photocatalytic efficiency. Mechanistic investigations on modified TiO_2 systems have demonstrated that surface and interfacial interactions significantly influence charge separation behavior and photoactivity (Sudrajat et al., 2022; Sudrajat & Hartuti, 2026).

Integrated Mechanism Summary

Overall, the TiO_2–coal fly ash system can be interpreted as an integrated photocatalytic platform enabling two coupled redox pathways operating simultaneously at the catalyst surface: (1) oxidative degradation of organic compounds in greywater driven by photogenerated holes and hydroxyl radicals, and (2) reductive hydrogen evolution driven by conduction-band electrons whose availability is enhanced by the hole-scavenging activity of organic species. The coal fly ash support contributes to both pathways by improving pollutant adsorption and catalyst stability. A schematic illustration of the proposed integrated mechanism is presented in **Figure 6**.

3.5. Research Limitations and Future Directions

This study provides preliminary baseline performance data for a TiO_2–coal fly ash photocatalytic system operating with real laundry greywater. Several limitations of the current study are acknowledged and should be addressed in future work.The absence of negative control experiments (UV irradiation without catalyst; catalyst without UV irradiation) prevents definitive attribution of the measured organic removal to photocatalytic activity alone, as contributions from direct photolysis and adsorption cannot be separately quantified. Future studies should include full factorial control experiments to isolate each degradation pathway.

The chemical identity of the gas detected by the MQ-2 sensor has not been verified. The sensor response establishes only the presence of a reducing gas in the headspace; hydrogen is the most plausible attribution

based on thermodynamic arguments and system conditions, but volatile organic stripping and biogenic gas formation cannot be formally excluded. Future work must employ GC-TCD or GC-MS analysis for definitive chemical identification and precise quantification of gas products. Until such confirmation is obtained, the term 'hydrogen evolution' used in this manuscript refers to a preliminary, qualitative observation rather than a verified chemical event.

Hydrogen identification in this study remains qualitative, based on semiconductor sensor response, and has not been verified by quantitative gas chromatography. Future work should employ GC-TCD analysis for precise determination of hydrogen production rates and selectivity.

Post-synthesis characterization of the TiO_2–coal fly ash composite was not performed in this study, representing a significant methodological limitation. The formation of crystalline TiO_2 on the coal fly ash surface has not been directly verified; all structural inferences are based on precursor properties and synthesis conditions. Advanced characterization, including XRD for anatase phase identification, SEM-EDX for surface morphology and Ti distribution, BET for specific surface area, FTIR for surface functional groups, and UV-Vis DRS for optical band gap determination, is designated as a mandatory component of the subsequent research phase before any performance optimization or scale-up can be meaningfully pursued. Additionally, post-reaction TSS measurement, ultrasonic adhesion testing, ICP-OES determination of dissolved Ti in the effluent, and coating mass-loss measurement across repeated reuse cycles are identified as necessary components of future work to verify coating stability and exclude the possibility of catalyst leaching into the treated effluent.

Finally, systematic optimization of key operational parameters, including UV lamp intensity and wavelength, initial pH of greywater, catalyst loading, and reaction time, is necessary to establish the conditions required for maximum photocatalytic performance, and represents the logical next step in the development of this integrated system toward practical application at household or communal scales.

A critical safety consideration that was not addressed in the present study is the potential leaching of toxic trace elements, particularly arsenic (As), lead (Pb), cadmium (Cd), and chromium (Cr), from the coal fly ash support into the treated greywater effluent during photocatalytic operation. This omission represents an important limitation, particularly given that the Introduction of this manuscript explicitly cites arsenic mobilization from coal fly ash in the presence of dissolved organic matter as an environmental concern. Although the acid-washing pretreatment (0.1 M HCl) applied prior to synthesis is expected to remove a substantial fraction of surface-associated leachable species, and although the fly ash was immobilized within a calcined TiO_2 matrix rather than dispersed freely, these factors reduce but do not eliminate leaching risk under the acidic-to-neutral pH and organic-rich conditions of the photocatalytic experiment. Determination of trace element concentrations in the treated effluent by ICP-OES or atomic absorption spectroscopy (AAS) is therefore designated as a mandatory prerequisite before any scale-up or field application of this system. Until such verification is completed, the treated effluent should not be considered safe for discharge or reuse, and the technology described here should be regarded as a laboratory-stage proof of concept only.

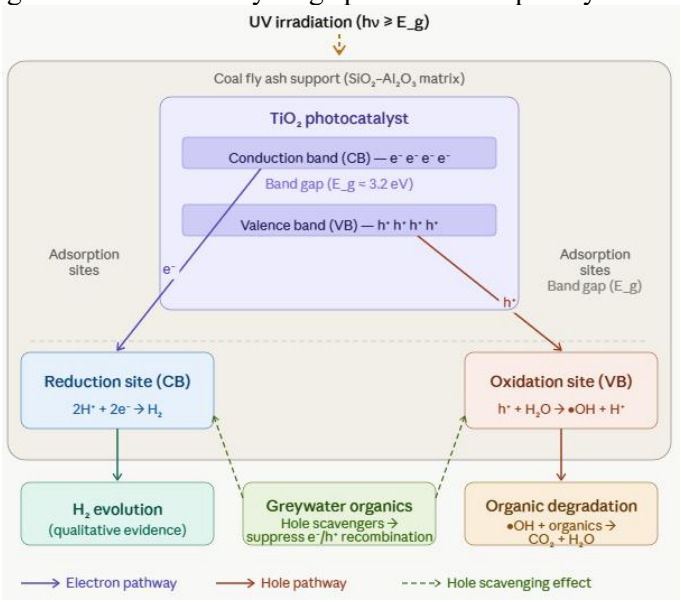


Figure 6. Proposed integrated photocatalytic mechanism of the TiO_2–coal fly ash system: simultaneous oxidative organic degradation and reductive hydrogen evolution using laundry greywater as the reaction medium and hole scavenger.

4. CONCLUSION

This study demonstrated the technical feasibility of valorizing coal fly ash as a low-cost support material for TiO_2-based photocatalysts synthesized via a sol–gel method, evaluated for simultaneous organic pollutant removal and hydrogen evolution using real laundry greywater as the reaction medium.

Physicochemical characterization of the coal fly ash confirmed its suitability as a photocatalyst support material, as evidenced by a low LOI value of 1.66%, a stable silica–alumina-dominated composition (SiO_2: 47.64%; Al_2O_3: 18.17%), and a slurry pH successfully reduced from 11.25 to approximately 8.0 following the applied pretreatment protocol. These characteristics support the suitability of coal fly ash as a precursor support material; however, direct verification of TiO_2 layer formation on the composite surface was not performed in this study, and XRD, SEM-EDX, BET, and UV-Vis DRS analyses are identified as mandatory steps for the subsequent research phase.

Six hours of UV irradiation of real laundry greywater achieved a mean apparent overall system removal efficiency of 53.96 ± 0.12% ($p < 0.001$), reducing the permanganate index from 97.90 ± 0.01 mg/L to 45.08 ± 0.12 mg/L. This result indicates that the integrated TiO_2–coal fly ash system is functionally capable of lowering the dissolved organic load of complex real greywater under non-optimized baseline conditions, although the relative contributions of photocatalysis, photolysis, and adsorption remain to be resolved through control experiments. Qualitative evidence of reducing gas formation, consistent with photocatalytic hydrogen evolution, was detected using a semiconductor-based MQ-2 gas sensor under nitrogen-purged anaerobic conditions, suggesting the concurrent operation of oxidative and reductive pathways within the photocatalytic system — with organic compounds in greywater functioning simultaneously as degradation targets and as hole scavengers that suppress electron–hole recombination and enhance electron availability for proton reduction.

The proposed integrated mechanism positions the TiO_2–coal fly ash system as a dual-function photocatalytic platform capable of simultaneous wastewater treatment and clean energy generation, with coal fly ash serving as a locally abundant and low-cost industrial by-product in Indonesia that can be valorized as a functional catalyst support material.

These findings provide baseline performance data for the development of low-cost, dual-function photocatalytic systems applicable at household or communal scales. Future work should prioritize: (1) quantitative hydrogen production analysis by gas chromatography (GC-TCD); (2) advanced material characterization including XRD phase analysis, BET surface area measurement, and FESEM morphological analysis of the TiO_2–coal fly ash composite; (3) negative control experiments to isolate photocatalytic, photolytic, and adsorptive contributions to organic removal; and (4) systematic optimization of operational parameters including UV irradiation intensity, catalyst loading, initial greywater pH, and reaction time, toward the development of a practically applicable and scalable photocatalytic greywater treatment system.

CONFLICT OF INTEREST

The authors gratefully acknowledge the financial support from Institute of Technology Padang (Grant No. 84/27.O10.1.2/PN/VIII/2025). The authors express their gratitude to Jhim Redi, Quality Control Manager at PT. Semen Padang, Indonesia, for providing the sample and for his technical assistance in X-ray fluorescence (XRF) analysis. The authors also acknowledge the support and access to laboratory facilities provided by the Department of Environmental Engineering and the Department of Civil Engineering, Institute of Technology Padang.

REFERENCES

ASTM International. (2022). Standard specification for coal fly ash and raw or calcined natural pozzolan for use in concrete (Standard No. C0618-22). https://doi.org/10.1520/C0618-22

Aslam, M., Bin Fazal, D., Ahmad, F., Bin Fazal, A., Abdullah, A. Z., Ahmed, M., Qamar, M., & Rafatullah, M. (2022). Photocatalytic degradation of recalcitrant pollutants of greywater. Catalysts, 12(5). https://doi.org/10.3390/catal12050557

Badan Standarisasi Nasional. (2004). SNI 06-6989.22: Air dan air limbah — Bagian 22: Cara uji nilai permanganat secara titrimetri. BSN.

Boyjoo, Y., Ang, M., & Pareek, V. (2012). Photocatalytic treatment of shower water using a pilot scale reactor. International Journal of Photoenergy, 2012, Article 578916. https://doi.org/10.1155/2012/578916

Deonarine, A., Kolker, A., Doughten, M. W., Holland, J. T., & Bailoo, J. D. (2021). Mobilization of arsenic from coal fly ash in the presence of dissolved organic matter. Applied Geochemistry, 128, 104950. https://doi.org/10.1016/j.apgeochem.2021.104950

Hartuti, S., Hanum, F. F., Takeyama, A., & Kambara, S. (2017a). Effect of additives on arsenic, boron and selenium leaching from coal fly ash. Minerals, 7(6). https://doi.org/10.3390/min7060099

Hartuti, S., Kambara, S., & Takeyama, A. (2017b). Arsenic leachability of coal fly ashes from different types of coal fired power plants. Journal of Materials Science and Engineering A, 7(7–8). https://doi.org/10.17265/2161-6213/2017.7-8.001

Hartuti, S., Kambara, S., Takeyama, A., & Hanum, F. F. (2017c). Leaching characteristic of arsenic in coal fly ash. Journal of Materials Science and Engineering B, 7(1–2). https://doi.org/10.17265/2161-6221/2017.1-2.003

Hartuti, S., Saleh, N., & Azatri, V. (2025). Coal fly ash beneficiation: A substitute material for Portland cement — A review. Journal of Infrastructural in Civil Engineering. https://doi.org/10.33365/jice.v6i02.689

Kanakaraju, D., Ya, M. H. B., Lim, Y.-C., & Pace, A. (2020). Combined adsorption/photocatalytic dye removal by copper-titania-fly ash composite. Surfaces and Interfaces, 19, Article 100534. https://doi.org/10.1016/j.surfin.2020.100534

Li, X., Lin, S., & Hu, R. (2025). Recent progress in visible-light photocatalysts materials: Synthesis, applications, challenges, and prospects. Journal of Pure and Applied Chemistry Research. https://doi.org/10.47852/bonviewJOPR52023222

Lu, C. G., Jiao, C. J., Zhang, X. C., Lin, W. C., & Chen, X. F. (2025). Fly ash-supported photocatalysts: Synthesis, applications, and advances in modification technology. Crystals, 15(3). https://doi.org/10.3390/cryst15030223

Maaß, M. C., Tasch, A., Jooss, C., & Waitz, T. (2022). Photocatalytic hydrogen evolution using ZnS particles and LEDs. Journal of Chemical Education, 99(5), 2086–2092. https://doi.org/10.1021/acs.jchemed.1c01157

Mohan, S., Manthapuri, V., & Chitthaluri, S. (2024). Assessing factors influencing greywater characteristics around the world: A qualitative and quantitative approach with a short-review on greywater treatment technologies. Discover Water, 4(1). https://doi.org/10.1007/s43832-024-00094-w

Navidpour, A. H., Abbasi, S., Li, D., Mojiri, A., & Zhou, J. L. (2023). Investigation of advanced oxidation process in the presence of TiO_2 semiconductor as photocatalyst: Property, principle, kinetic analysis, and photocatalytic activity. Catalysts, 13(2). https://doi.org/10.3390/catal13020232

Sanchez, M., Rivero, M. J., & Ortiz, I. (2010). Photocatalytic oxidation of grey water over titanium dioxide suspensions. Desalination, 262(1–3), 141–146. https://doi.org/10.1016/j.desal.2010.05.060

Sanni, S. O., Pholosi, A., Pakade, V. E., & Brink, H. G. (2025). Adsorptive and photocatalytic remediation of greywater in wastewater: A review. Adsorption, 31(3), 58. https://doi.org/10.1007/s10450-025-00607-6

Sohibun, Maulana, F., & Fitriyanti. (2021). MQ-2 gas sensor using micro controller Arduino Uno for LPG leakage with short message service as a media information. Journal of Physics: Conference Series, 2049, 012068. https://doi.org/10.1088/1742-6596/2049/1/012068

Sudrajat, H., Babel, S., Hartuti, S., Phanthuwongpakdee, J., Laohhasurayotin, K., Nguyen, T. K., & Tong, H. D. (2021). Origin of the overall water splitting activity over Rh/Cr_2O_3@anatase TiO_2 following UV-pretreatment. International Journal of Hydrogen Energy, 46(61), 31228–31238. https://doi.org/10.1016/j.ijhydene.2021.07.002

Sudrajat, H., Hartuti, S., & Babel, S. (2022). Mechanistic understanding of the increased photoactivity of TiO_2 nanosheets upon tantalum doping. Physical Chemistry Chemical Physics, 24(2), 995–1006. https://doi.org/10.1039/d1cp03907e

Sudrajat, H., & Hartuti, S. (2026). Toward quantum science- and technology-enabled heterogeneous catalysis. Journal of Materials Chemistry A, 14, 9895–9938. https://doi.org/10.1039/D5TA08272B

Sudrajat, H., Susanti, A., & Hartuti, S. (2023). Reduced TiO_2 with prolonged electron lifetime for improving photocatalytic water reduction activity. Journal of Physics: Condensed Matter, 35(13). https://doi.org/10.1088/1361-648X/acb4d2

Wu, Y., Li, Y., Hu, H., Zeng, G., & Li, C. (2021). Recovering hydrogen energy from photocatalytic treatment of pharmaceutical-contaminated water using Co_3O_4 modified {001}/{101}-TiO_2 nanosheets. ACS ES&T Engineering, 1(3), 603–611. https://doi.org/10.1021/acsestengg.1c00003

Xie, Y., Xu, C., Liu, Y., Zhang, E., Chen, Z., Zhan, X., Deng, G., Gao, Y., & Zhang, Y. (2025). Photothermal synergistic hydrogen production via a fly-ash-made interfacial vaporific system. Advanced Science, 12(3). https://doi.org/10.1002/advs.202410201

Zhang, X., Cheng, Z., Bo, C., Sun, Y., & Piao, L. (2025). The photocatalytic wastewater hydrogen production process with superior performance to the overall water splitting. Journal of Colloid and Interface Science.